

An anomalous alloy: Y_xSi_{1-x}

V. Meregalli, M. Parrinello
 Max-Planck-Institut für Festkörperforschung
 Heisenbergstrasse. 1, D-70569 Stuttgart, Germany
 (November 20, 2018)

We study via density functional-based molecular dynamics the structural and dynamical properties of the rare earth silicon amorphous alloy Y_xSi_{1-x} for $x = 0.093$ and $x = 0.156$. The Si network forms cavities in which a Y^{3+} cation is entrapped. Its electrons are transferred to the Si network and are located in the dangling bonds of the Si atoms that line the Y cavities. This leads to the presence of low coordinated Si atoms that can be described as monovalent or divalent anions. For $x = 0.156$, the cavities touch each other and share Si atoms that have two dangling bonds. The vibrational spectrum is similar to that of amorphous Si . However, doping induces a shoulder at 70 cm^{-1} and a pronounced peak at 180 cm^{-1} due to low coordinated Si .

Rare earth doped silicon alloys have received considerable attention due to their intriguing properties and for their potential in the applied domain. They show an interesting metal-insulator transition and their optical conductivity exhibits apparent sum rule violations [1], as in manganates and high T_c compounds. In addition Gd_xSi_{1-x} alloys have an enormous negative magneto-resistance [2] and spin-glass behaviour has been reported [3]. In spite of a large number of experimental investigations the structure of this and related compounds is still a matter of guesswork. For this reason we have undertaken here an *ab-initio* molecular dynamics investigation of the Y_xSi_{1-x} alloy. This is non-magnetic but has electronic structure properties that set it apart from all the other amorphous Si alloys so far studied.

In our simulation we followed the method of Car and Parrinello [4] as implemented in the CPMD code [5]. Local density approximation and norm-conserving Goedecker-type pseudopotentials have been used [6], [7] (for Y the semi-core 4d states have been included in the valence). The simulation cell is a cube of length 11.216 Å containing a total of 64 atoms. Periodic boundary conditions are applied. The concentrations $x = 0.093$ ($58Si + 6Y$) and $x = 0.156$ ($54Si + 10Y$) have been studied. The Car-Parrinello equations of motion with a fictitious electronic mass of 400 a.u. were integrated using a time step of 3 a.u. (0.072 fs). In order to generate the amorphous structure we used the following procedure. We start from a cubic lattice with the Y atoms placed randomly, but as far as possible from one another. Such an unlikely configuration is rapidly destroyed and leads to fast melting. The system is kept in this liquid state at the temperature of 1650 K for about 0.35 ps, in order to lose memory of the initial condition. Then the temperature is brought down to 300 K in a time span of 0.3 ps.

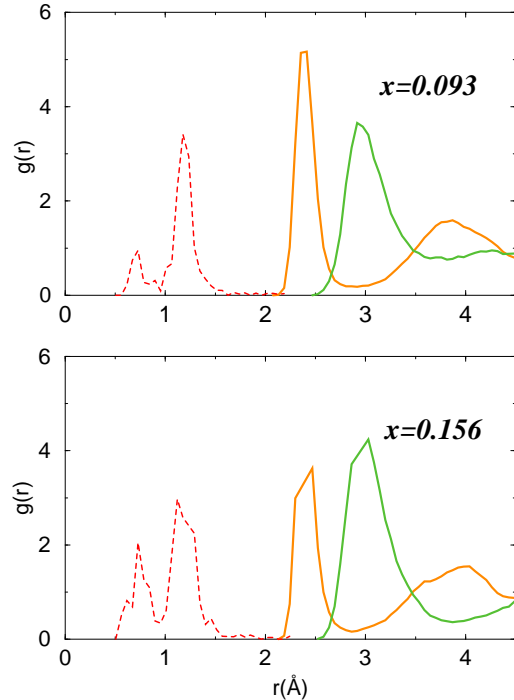


FIG. 1. $Si - Si$ (orange line), $Si - Y$ (green line) and $Si - WFCs$ (red line) pair correlation functions for both the concentrations. The data have been obtained by averaging over all the configurations of the molecular dynamics simulations. The $Si - WFCs$ correlation function has been scaled by a factor of 3.

Although the annealing rate is rather fast, past experience in semiconducting alloys has shown that the main features of the amorphous structure are well reproduced [8]. The system was finally allowed to evolve at 300 K for 10 ps without ionic temperature control. The system is a metal in the liquid state and a small gap semiconductor when amorphous at room temperature. In the annealing part of the run we controlled the fictitious electronic kinetic energy drift by periodic quenches to the Born Op-

penheimer surfaces. Instead a Nose’ thermostat was used for the electrons in the last 10 ps. The thermostat characteristic frequency was 1500 cm^{-1} and the target electronic fictitious kinetic energy was set according to the prescription of reference [9]. The vibrational spectrum and other statistical averages were evaluated during the last 10 ps.

In Fig. 1 we report the measured correlation functions g_{SiSi} and g_{YSi} . Due to the small number of atoms the g_{YY} ’s are very noisy and are not reported in order not to clutter the figure. However they show a strong tendency for the Y to repel each other. From the correlation functions as well as a visual inspection of the structure we could infer that Si atoms tend to form a tetrahedrally bonded amorphous network as in pure $a-Si$. However Y atoms are not part of the Si amorphous network but sit at the centre of cavities. In order to accommodate these cavities the Si network has to generate a number of under-coordinated Si atoms in the proximity of the Y impurities.

A very valuable help in understanding the electronic properties of amorphous structures is provided by the maximally localised Wannier functions [10] and their centres, as discussed in ref. [11] for the case of pure $a-Si$. Wannier functions are obtained from the Kohn and Sham orbitals by performing a unitary transformation that minimises the average orbital spread. The resulting orbitals capture the chemical nature of the bond. An even simpler and more vivid picture is obtained by considering only their centroids.

This is demonstrated in Fig. 1 where we plot the Si Wannier centre correlation functions. The first peak is split into two. The higher peak is centred at half of the $Si-Si$ bond distance and clearly reflects the formation of the covalent bond. There is, however, a very sizable peak at shorter distances which is due to the presence of dangling bonds, whose height increases with Y concentration. Since these peaks are well separated we can classify the Wannier centre and the corresponding Wannier functions into “covalent” and “dangling”. The different nature of these classes of functions is reflected also in their spread distribution, which is bimodal with peaks centred at $\sim 1.5\text{ \AA}$ and $\sim 1.85\text{ \AA}$ for “covalent” and “dangling” bonds respectively.

As in ref. [11] we can identify the covalently bonded $Si-Si$ atoms as those pairs of atoms which share “covalent” Wannier functions. Using this criterion, which is based on the chemistry of the system and not simply on a geometric distance consideration, we find that in the Si network there are twofold, threefold and fourfold-coordinated atoms. As a function of the concentration, due to the need to accommodate more Y impurities, the number of threefold-coordinated silicons increases noticeably (from 20% to 40%) while that of fourfold-coordinated atoms decreases (from 70% to 50%). We also noticed an increase of the twofold-coordinated silicons; however, due

to the limited statistics we do not attempt to define here the probability of their occurrence.

In Fig. 2 we show two typical environments for the Y atoms. At the higher concentration the Y atoms have to share some of their first neighbours. These shared Si atoms tend to be twofold coordinated as shown in the picture. Finally the Wannier analysis shows clearly that Y has lost all its valence electrons and is in the oxidation state $3+$. Thus the picture that emerges from our simulation is one in which the Y atoms donate their valence electrons to the Si sub-lattice. These electrons are then stored in the Si network and localised in the doubly occupied dangling bonds of the threefold and twofold coordinated Si atoms. These atoms are therefore negatively charged and can be thought of as being a realization of the species Si^- and Si^{--} . These species tend to cluster around the Y cation, not only to form the cavity in which the impurity sits but also to ensure local charge neutrality. As such they are an integral part of the structure. The silicon dangling bonds provide the ligand field to the metal ion.

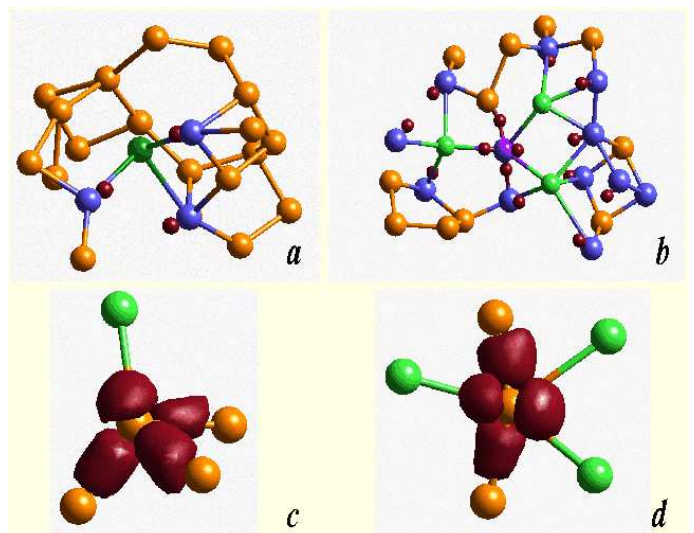


FIG. 2. Snapshots of two configurations of the molecular dynamics simulation for both concentrations $x = 0.093$ (a) and $x = 0.156$ (b). Fourfold-coordinated silicon atoms are represented in orange, threefold-coordinated in blue, twofold-coordinated in purple, yttrium atoms in green and lone-pair Wannier centres in red. For clarity only the lone-pair Wannier centres have been plotted. Below each configuration we have plotted the Wannier function density $\rho_n(\mathbf{r}) = |w_n(\mathbf{r})|^2$, for one of the threefold-coordinated atoms above (c) and for the twofold-coordinated atom above (d).

In Fig. 3 we show the vibrational density of states analysed in the contributions from the species Y , Si and Si^- . The general appearance of the spectrum is very similar to that of pure $a-Si$. However, we note a shoulder $\sim 70\text{ cm}^{-1}$ which is due to the Y atoms; we also note that, especially for $x = 0.156$, the Si^- make an important contribution and together with the Y alter the relative

intensities of the peaks. Since Si^- is expected to have a higher infra-red activity than Si we can predict that the infra-red spectrum will show an enhancement of the 180 cm^{-1} peak, and a Y related structure at 70 cm^{-1} . The intensities of either peak should increase as a function of x .

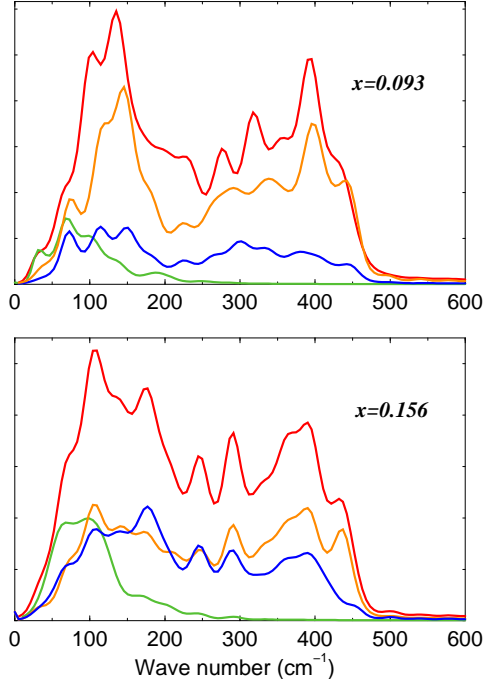


FIG. 3. Total vibrational spectrum (red line) together with its contributions from Y (green line), four-fold-coordinated Si (orange line) and threefold-coordinated Si (blue line), for $x = 0.093$ (upper panel) and $x = 0.156$ (lower panel).

For a selected small number of configurations we evaluated the HOMO-LUMO gap. This shows large oscillations in the range 0.2 to 0.45 eV .

In Fig. 4 we show the total electronic density of states (DOS) and its projection on the covalent and dangling Wannier functions. These show clearly that the dangling states dominate the electronic DOS close to the Fermi level.

These two facts are not in contradiction to a picture in which the conductivity takes place via an hopping mechanism as suggested by the experiments.

In conclusion, we have shown that Y_xSi_{1-x} alloys at low concentrations have a very peculiar electronic structure. The Y donates its valence electrons to the Si network and is trapped in cavities. These electrons are trapped in doubly occupied Si dangling bonds. These defect states can be observed via infra-red spectroscopy. Our study can be a stepping stone for the more complex case of the magnetic $4d$ alloys. In fact it is likely that many of the features found here will also be present in the

case of Gd and contribute to its unusual properties. We could speculate that as the Y concentration increases the Y filled cavities interact more and more until the tetrahedrally bonded network of Si is disrupted and local coordinations like those observed in the stoichiometric compound YSi_2 will dominate the local structure. We plan to address these issues in our forthcoming work.

We thank M. Bernasconi, P. L. Silvestrelli and F. Hellman for stimulating discussions.

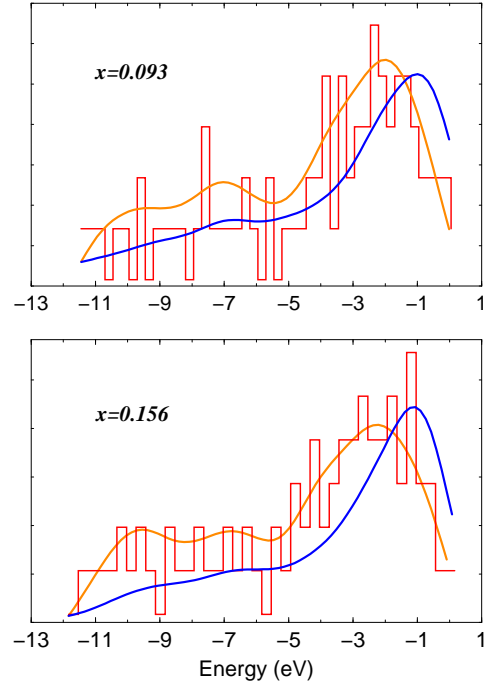


FIG. 4. Electronic density of states (red line) and its projection on the covalent (orange line) and dangling (blue line) Wannier functions. Note that the projection are not normalised and the Fermi level defines the zero of the energy.

-
- [1] F. Hellman, M. Q. Tran, A. E. Gebala, E. M. Wilcox and R. C. Dynes, Phys. Rev. Lett. **77**, 4652 (1996)
 - [2] B. L. Zink, E. Janod, K. Allen and F. Hellman, Phys. Rev. Lett. **83**, 2266 (1999)
 - [3] P. Xiong, B. L. Zink, S. I. Applebaum, F. Hellman and R. C. Dynes, Phys. Rev. B **59**, 3929 (1999)
 - [4] R. Car and M. Parrinello, Phys. Rev. Lett. **55**, 2471 (1985).
 - [5] CPMD, J. Hutter et. Al. MPI für Festkörperforschung and IBM Zurich Research Laboratory 1995 - 1999.
 - [6] S. Goedecker, M. Teter and J. Hutter, Phys. Rev. B **54**, 1703 (1996).
 - [7] C. Hartwigsen, S. Goedecker and J. Hutter, Phys. Rev. B **58**, 3641 (1998).

- [8] R. Car and M. Parrinello Phys. Rev. Lett. **60**, 204 (1988); G. Galli, R. M. Martin, R. Car and M. Parrinello, Phys. Rev. Lett. **62**, 555 (1989); F. Buda, G. L. Chiarotti, I. Stich, R. Car and M. Parrinello, J. Non-Cryst. Solids **114**, 7 (1989); G. Galli, R. M. Martin, R. Car and M. Parrinello, Phys. Rev. B **44**, 11092 (1991); F. Finocchi, G. Galli, M. Parrinello and C. M. Bertoni, Phys. Rev. Lett. **68**, 3044 (1992); N. A. Marks, D. R. McKenzie, B. A. Pailthorpe, M. Bernasconi and M. Parrinello, Phys. Rev. Lett. **76**, 768 (1996); A. Gambirasio M. Bernasconi, Phys. Rev. B **60**, 12007 (1999); D. G. McCulloch, D. R. McKenzie and C. M. Goringe, Phys. Rev. B **61**, 2349 (2000).
- [9] P. E. Blöchl and M. Parrinello, Phys. Rev. B **45**, 9413 (1992).
- [10] N. Marzari and D. Vanderbilt, Phys. Rev. B **56**, 12847 (1997).
- [11] P. L. Silvestrelli, N. Marzari D. Vanderbilt and M. Parrinello, Sol. State. Comm. **107**, 7 (1998).